Seismic probabilistic risk assessment of weir structures considering the earthquake hazard in the Korean Peninsula

Jahangir Alam[1a], Dookie Kim[*1] and Byounghan Choi[2b]

[1]*Civil and Environmental Engineering, Kunsan National University, 558 Daehak-ro, Gunsan-si 54150, Republic of Korea*
[2]*Rural Research Institute, 870, Haean-ro Sangnok-gu, Ansan-si Gyeonggi-do, 15634, Republic of Korea*

Abstract.   Seismic safety evaluation of weir structure is significant considering the catastrophic economical consequence of operational disruption. In recent years, the seismic probabilistic risk assessment (SPRA) has been issued as a key area of research for the hydraulic system to mitigate and manage the risk. The aim of this paper is to assess the seismic probabilistic risk of weir structures employing the seismic hazard and the structural fragility in Korea. At the first stage, probabilistic seismic hazard analysis (PSHA) approach is performed to extract the hazard curve at the weir site using the seismic and geological data. Thereafter, the seismic fragility that defines the probability of structural collapse is evaluated by using the incremental dynamic analysis (IDA) method in accordance with the four different design limit states as failure identification criteria. Consequently, by combining the seismic hazard and fragility results, the seismic risk curves are developed that contain helpful information for risk management of hydraulic structures. The tensile stress of the mass concrete is found to be more vulnerable than other design criteria. The hazard deaggregation illustrates that moderate size and far source earthquakes are the most likely scenario for the site. In addition, the annual loss curves for two different hazard source models corresponding to design limit states are extracted.

Keywords: seismic risk assessment; weir structure; seismic fragility; seismic hazard analysis; annual loss

1. Introduction

The weir structures are critical lifeline infrastructure that usually serves to control the flood, generation of electric power, water supply, irrigation and recreation purposes. The seismic risk assessment of weir structure is particularly important considering the economic losses due to disruption of its operation and maintenance. Recently, the risk assessment and disaster management of critical hydraulic infrastructure have been issued due to the increased frequency of earthquake and flood for the effect of climate change in Korea. Many researchers are performing seismic fragility analysis for risk evaluation of concrete dams and weir structures. For example, Hariri-Ardebili and Saouma (2016) provided a methodology for vulnerability assessment of concrete dam and showed the important factors for probabilistic assessment of dams. Tekie and Ellingwood (2003) came up with a framework for developing fragility of concrete gravity dam to evaluate the seismic performance. Arefian *et al.* (2016) analyzed the seismic vulnerability of a cemented material dam based on the length and area of the crack created at the base of the dam as failure criteria. Ju and Jung (2015) evaluated the fragility of weir structure in Korea considering the limit states as compressive stress, tensile stress, and displacement. Also,

the effect of near source and far source ground motion were considered. In case of seismic structural fragility analysis, people are using different probabilistic approach. For example, the building damage functions were developed considering the quantitative measures of ground shaking for the loss estimation of the structure (Kircher *et al.* 1997). Pagni and Lowes (2006) developed a fragility function to predict the method of repair required for older reinforced concrete beam-column joints damaged due to earthquake loading. Porter *et al.* (2006) showed the analysis of damage data to create and test fragility functions for building components. Alam *et al.* (2017) showed a way to reduce uncertainty of seismic fragility using Bayesian inference with the help of markov chain monte carlo (MCMC) simulation. The seismic vulnerability analysis of highway bridges in Nepal was depicted, and the comparison between the constructed fragility curves with other observational fragility curves was shown (Gautam 2017).

Although the Korea is known as a low and moderate earthquake seismicity region (Choi *et al.* 2005), recently, more frequent and bigger earthquakes have been observed. The Gyeongju earthquake was the largest recorded earthquake on the Korean Peninsula with magnitude 5.8, and which was occurred on September 12, 2016. In addition, another recent earthquake was recorded with magnitude 5.4, called Pohang earthquake, on November 15, 2017. Therefore, the significance of seismic risk evaluation of critical infrastructures (i.e., dams, weirs, bridges and others) by considering the site-specific hazard is growing up for engineers. Zimmaro and Stewart (2017) performed the site-specific probabilistic seismic hazard analysis for Calabrian dam site in Southern Italy and compared the prior

---

∗Corresponding author, Professor
 E-mail: kim2kie@kunsan.ac.kr
[a]Master Student
[b]Ph.D.

Table 1 Material properties of the weir structure

Structures	Modulus of Elasticity (MPa)	Poisson's ratio	Unit weight (Kg/m^3)
Weir Body	26637	0.167	2400
Mass Concrete	24579	0.167	2400
Soil Layer 1	2	0.4	1700
Soil layer 2	25	0.4	1900
Soil Layer 3	2000	0.3	2400

uniform hazard spectrum to his study. The probabilistic seismic hazard analysis (PSHA) approach was performed for two cities of Iran, and attenuation equation and uniform hazard spectra (UHA) was developed based on two customary hazard level (Alireza and Kamali-Asl 2015). A comprehensive framework for seismic risk and loss estimation was developed considering the seismic hazard and fragility, and demonstrated for two cities of Greek and Turkish (Pitilakis *et al.* 2011). In addition, the seismic hazard analysis was performed at the Itoiz dam site, Spain; and the framework for seismic performance of dam was provided (Garcia-Mayordomo and Insua-Arevalo 2011). Gautam *et al.* (2016) showed the site response analysis and associated structural damage analysis of five location in Kathmandu Valley, Nepal. Recently, Choi *et al.* (2009) performed PSHA method for nuclear power plant site in Korea and developed site-specific uniform hazard spectrum. The seismic source models were proposed by using historical and instrumental earthquake. However, limited guidance is available for the seismic risk assessment of hydraulic structures considering the site-specific hazard analysis in Korea.

The study examines probabilistic dependence prospect of earthquake risk of the weir structure by considering the seismic hazard source data in Korea. The PSHA method is employed to assess the seismic hazard of the weir site. The most probable earthquake scenarios of the site are shown by hazard deaggregation. The 2D finite element model (FEM) of weir structure together with the soil-structure foundation is used to perform numerical analysis for developing the seismic fragility. The evaluation can have important implications regarding the performance of the structures and regional impacts. After all, the seismic risk is analyzed by the convolution of seismic fragility and hazard function.

2. Structural analysis

2.1 Weir structure model

The Gangjeong-Goreyeong weir structure, located on the Nakdong River in Korea was constructed due to the irrigation and hydropower generation purposes (Ju and Jung 2015). The overall length of the concrete weir structure is 933.5m consisting of overflow and non-overflow section. The height of the weir section is 11.03 m and storage capacity is 92.3 million m^3. The weir structure is modeled considering the three different soil foundations layers (i.e., layer 1: sand, layer 2: gravel-sand mixture and layer 3: rock). Fig. 1 illustrates the details dimension of the weir
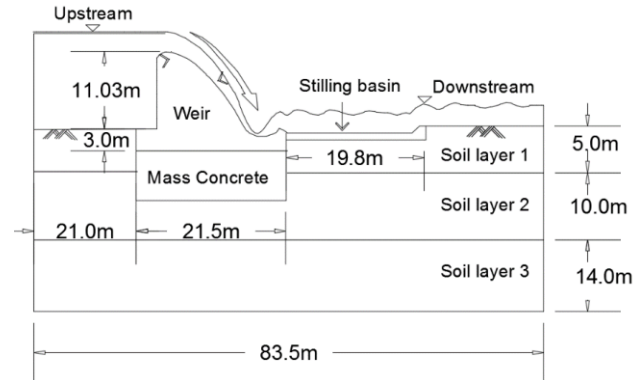

Fig. 1 The geometry of Gangjeong-Goreyeong weir structure
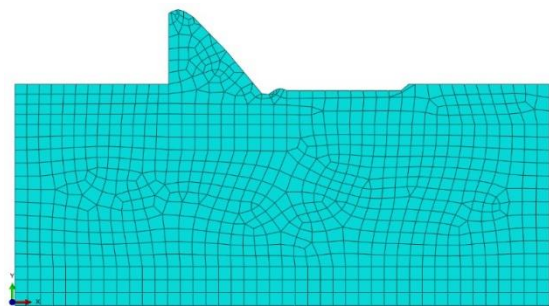

Fig. 2 2D FE model of Gangjeong-Goreyeong weir structure

structure. The material properties of weir structure are shown in Table 1 (Ju and Jung 2015). For numerical analysis of weir structure, 2D FEM is generated by using ABAQUS as shown in Fig. 2. The concrete design strength of weir and mass concrete are 24 MPa and 18 MPa respectively.

2.2 Load consideration

For structural analysis of weir structure, four different loadings (hydrostatic pressure, hydrodynamic pressure, uplift pressure and silt pressure) are considered with earthquake and self-weight. The hydrostatic pressure generally varies due to increasing the height of water and can be calculated by the following equation

$$P_w = \rho g h \tag{1}$$

where ρ is the density of water, g is the acceleration of gravity (9.81m/s^2), and h is the depth of water.

In the field of the hydraulic structure, the Westergaard equation is commonly accepted for estimating the hydrodynamic pressure on the rigid reservoir dam (Karaca and Küçükarslan 2012). The governing equation is as follows

$$P_d = 0.875\rho_w g k \sqrt{H \times h} \tag{2}$$

where P_d is the hydrodynamic pressure (MPa), k is the design seismic coefficient which is two third of the peak ground acceleration in term of g (i.e., 0.67(PGA/g)), H is total height of the water, and h is height from water level to the calculating point.
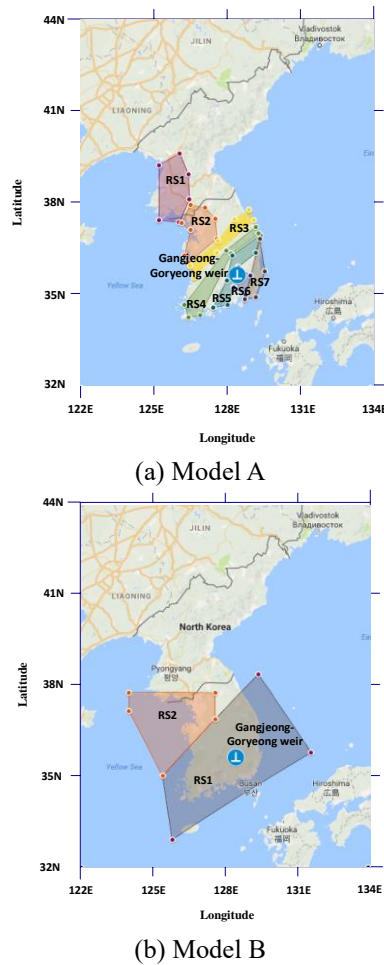
(a) Model A

(b) Model B

Fig. 3 Seismic source maps for probabilistic seismic hazard analysis

Table 2 Seismicity parameters of the seismic source maps

| Source model | Zone | Seismicity parameters | | Max. Magnitude | Min. Magnitude |
		a	b		
Model A	RS1	4.28	1.12	6.6	
	RS2	3.53	0.92	6.9	
	RS3	2.59	0.69	7.1	
	RS4	2.34	0.66	6.7	3.8
	RS5	3.10	0.87	7.1	
	RS6	2.12	0.66	6.7	
	RS7	1.70	0.59	7.2	
Model B	RS1	2.93	0.76	6.7	3.0
	RS2	2.53	0.75	6.5	

zone because of no strong earthquake record was measured. Moreover, no active faults were identified in Korea. So, the Poisson type PSHA approach is exercised in Korea where all earthquakes are presumed to occur under a stationary process in the time domain (Choi *et al.* 2005). Recently, the seismology expert teams have been introduced the earthquake hazard source map for the PSHA, based on historical and instrumental earthquake data without a distinct seismo-tectonic environment. The seismic source model was developed by using more than 2000 earthquake data, in which more than 1800 earthquake data had been taken from the historical earthquake records (Seo *et al.* 1999). Seismic source models of Korea are shown in Fig. 3 that is used in this research. The distribution of the earthquake size was presumed to follow the Gutenberg-Richter recurrence law (Gutenberg and Richter 1944) and the hypocenters were assumed to be distributed uniformly and randomly. Table 2 shows the seismicity parameters for the seismic source model provided by CRIEPI (2006).

3.2 Probabilistic seismic hazard analysis

The rate of exceedance of a specific value of x of earthquake intensity measure (IM) can be calculated by using PSHA method. Generally, PSHA can consider the aleatory uncertainties of earthquake magnitude (M), source to site distance (R) and wave attenuation (McGuire, 1976).

$$\lambda(IM > x) = \sum_{i=1}^{N_S} \nu_i \sum_{j=1}^{N_M} \sum_{k=1}^{N_R} P(IM > x|m_j, r_k)P(M_i = m_j)P(R_i = r_k) \tag{5}$$

where ν_i indicates annual rate of earthquake occurrence which is provided by Gutenberg and Richter (1944).

$$\nu_i = 10^{a-bm_i} \tag{6}$$

where a and b values are known as the Gutenberg-Richter recurrence parameters. The resulting probability distribution of magnitude for the Gutenberg-Richter law can be determined by the ratio between the number of earthquake in a magnitude range prescribed to the total number of earthquakes (MacGuire 1976, 1978).

The uplift pressure reduces the effective weight of the structure, and therefore the restoring force is reduced. The uplift pressure can be expressed as (Ju and Jung 2015).

$$U = \gamma_w \times C \times A \times [H_2 + (H_1 - H_2) \times \tau] \tag{3}$$

where C is area ratio of contact surface, A is bottom area of contact pressure, H_1 is the upstream height of the dam weir, H_2 is the downstream height of the weir structure, and τ measure the ratio of $H_1 - H_2$ based on cut-off grouting and drainage curtain.

In addition, the earth pressure, silt pressure is taken into account in this study. The force of the silt pressure can be calculated using Rankine formula (Ali *et al.* 2012).

$$P_s = \gamma_{sub} K_a H^2 \tag{4}$$

where H is the height of the silt deposition, K_a means the coefficient of the active earth pressure of silt, and γ_{sub} defines the unit weight of silt materials.

3. Seismic hazard analysis

3.1 Seismic source map in Korea

Korea is recognized as a low and moderate seismicity

$$P(m_1 \leq M < m_2 | m_0 \leq m_1, m_2 \leq m_{max})$$
$$= \frac{10^{-bm_1} - 10^{-bm_2}}{10^{-bm_0} - 10^{-bm_{max}}} \qquad (7)$$

where m_0 and m_{max} are the lower threshold magnitude and maximum magnitude. Therefore, the seismicity parameters (a, b, m_0, m_{max}) of each source model are pivotal part for probabilistic seismic hazard analysis (Wang *et al.* 2013).

Ground motion prediction model is generally developed using statistical regression of observed ground motion intensities. In this study, predictive model of Cornell *et al.* (1979) is used for the mean of log peak ground acceleration (in units of g).

$$\overline{\ln PGA} = -0.152 + 0.859M - 1.803\ln(R + 25) \qquad (8)$$

The seismic hazard deaggregation expresses the mean annual rate of exceedance for particular ground motion intensity at any specific site base on the different source and their magnitudes and distances (Kramer 1996, Baker 2013).

$$\lambda(IM > x, M = m, R = r) = P(M_i = m)P(R_i$$
$$= r \sum_{i=1}^{N_s} v_i P(IM > x | m_j, r_k) \qquad (9)$$

4. Seismic fragility analysis

Seismic structural fragility defines as the probability of failure, that the seismic demand placed on the structure (D) is greater than the capacity of structure (C) (Tadinada, 2012).

$$Seismic\,fragility = P[D \geq C | IM] = P[C - D \leq 0 | IM] \qquad (10)$$

The lognormal distribution is commonly used to represent the collapse fragility curve (Bradley and Dhakal 2008, Baker 2015) and is used in this study.

$$P(C | IM) = \phi\left(\frac{\ln IM - \ln \theta}{\beta}\right) \qquad (11)$$

where $P(C | IM)$ denotes the fragility function for ground motion IM, $\phi()$ denotes the standard normal cumulative distribution function(CDF), θ is the median value of the distribution function, and β denotes the logarithmic standard deviation or dispersion of $\ln IM$.

There are different methods for estimating the two main parameters θ and β of fragility curve based on lognormal model. The incremental dynamic analysis (IDA) method involves scaling each ground motion in a suite until it causes collapse of the structure (Vamvatsikos and Cornell 2002). The intensity measure of the ground motion is gradually increased and applied into the structural model until the collapse is occurred. Fragility parameters can be estimated from analyses data by taking logarithms of each ground motion's IM value associated with onset of collapse, and computing there mean and standard deviation (Ibarra & Krawinkler 2005). Let, M be the number of specimen tested to failure, i is the index of specimen ($i =$

1,2, ….. M and IM is the value associated with the beginning of collapse for the ith ground motion (Ang and Tang 2006).

$$\theta = exp\left(\frac{1}{M}\sum_{i=1}^{M} lnIM_i\right) \qquad (12)$$

$$\beta = \sqrt{\frac{1}{M-1}\sum_{i=1}^{M}\left(ln\frac{IM_i}{\theta}\right)^2} \qquad (13)$$

5. Seismic probabilistic risk assessment

In general, the seismic probabilistic risk assessment approach is used to quantify the potential damages loss due to future earthquakes and their probabilities of occurrence in a given period (Brabhaharan *et al.* 2005). In this study, the lognormally distributed loss measure method (Porter, 2016) is used for estimating the risk curve of a single structure. The risk curve of the weir structure is expressed as the percentage of probable loss (FEMA 2001, Kalantari 2012, Noroozinejad Farsangi *et al.* 2014). Seismic risk curve can be estimated by integrating the seismic hazard function and seismic fragility function with respect to the ground motion intensity.

$$R(y) = \int_{=0}^{\infty} -(1 - P(Y \leq y | IM = x))\frac{dG(x)}{dx} dx \qquad (14)$$

where Y is the uncertain degree of loss, x is a particular value of the ground motion intensity, $R(y)$ annual frequency with which loss of degree y is exceeded, $G(x)$ is the mean annual frequency of shaking exceeding intensity x and $P(Y \leq y | IM = x)$ is the cumulative distribution function of IM evaluated at y for given shaking x. Risk curve can be estimated by numerically integrating of the n discrete values of earthquake intensity x (Porter 2016).

$$R(y) = \sum_{i=1}^{n}\left(p_{i-1}(y)a_i\right.$$
$$-\frac{\Delta p_i(x)}{\Delta s_i}G_{i-1}\left(exp(m_i\Delta s_i)\left(\Delta s_i\right.\right.$$
$$\left.\left.-\frac{1}{m_i}\right) + \frac{1}{m_i}\right)\right) \qquad (15)$$

where

$$a_i = G_{i-1}(1 - exp(m_i\Delta s_i)) \qquad (16)$$

$$m_i = \frac{ln\frac{G_i}{G_{i-1}}}{\Delta s_i} \; for \; i = 1,2, \dots \dots n \qquad (17)$$

$$p_i(y) = P(Y \leq y | IM = x) = 1 - \phi\left(\frac{ln\left(\frac{y}{\theta(x_i)}\right)}{\beta(x_i)}\right) \qquad (18)$$

Table 3 Limit state of weir structure

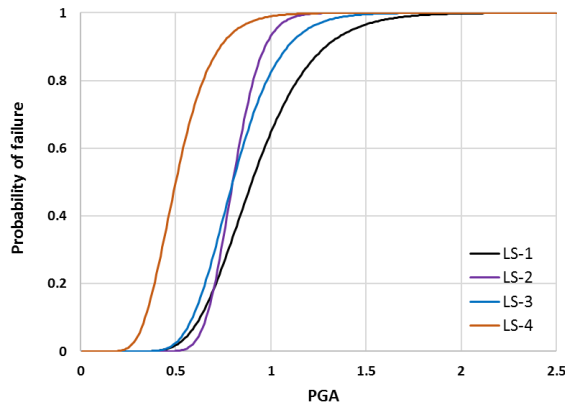| Limit States	Details	Design Criteria
LS-1	Compressive stress at weir body	$0.25f_{ck} = 6$MPa
LS-2	Tensile stress at weir body	$0.42\sqrt{f_{ck}} = 2.058$MPa
LS-3	Compressive stress at mass concrete	$0.25f_{ck} = 4.5$MPa
LS-4	Tensile stress at mass concrete	$0.42\sqrt{f_{ck}} = 1.782$MPa

Fig. 4 Seismic fragility curve of weir structure for the different limit state

6. Results and discussion

The 2D simple linear elastic plain strain EFM of weir structure is generated including three different soil layer to evaluate the seismic risk. For failure identification of the structure, four different limit state are considered based on design criteria of compressive stress and tensile stress of weir body and mass concrete (see Table 3). Thereafter, thirty-time history analyses are performed to assess the seismic fragility of the structure. From the numerical analysis results, fragility parameters are calculated by using IDA method for four different limit states. In case of IDA, fragility parameters are accounted by taking logarithms of each ground motion associated with the onset of collapse (Baker, 2015). From analyses results, the fragility parameters (θ, β) are estimated (0.90, 0.28), (0.81, 0.16), (0.79, 0.24) and (0.50, 0.30) for LS-1, LS-2, LS-3 and LS-4 respectively. Fig. 4 shows the seismic fragility curve of weir structure for four different limit state. From Fig. 4, we can see that the fragility curve for LS-2 are intersected with LS-1 and LS-3. It is because of the logarithmic standard deviation (β) value are less for LS-2. It means the slope of the lognormal fragility curve is very steep which indicates that the failure probability of structure change rapidly within a small interval of PGA value. The results illustrate that the failure probability of tensile stress of mass concrete (LS-4) is significantly greater than other failure criteria.

Using the seismic source maps as shown in Fig. 3, the probabilistic seismic hazard analyses are performed on the Gangjeong-Goreyeong weir structure site. Fig. 5 illustrates the PGA seismic hazard curve for the weir structure site. As shown in this figure, the PGA hazard curves from two different source models show a large variation of hazard. For example, the PGA values for the 10% exceedance
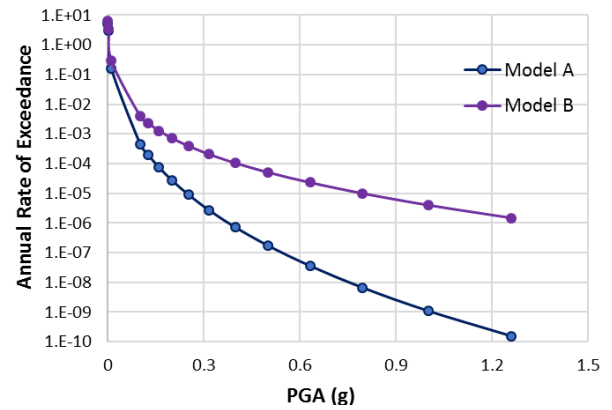

Fig. 5 PGA seismic hazard curve for the weir structure site located at 35.843ºN and 128.465ºE
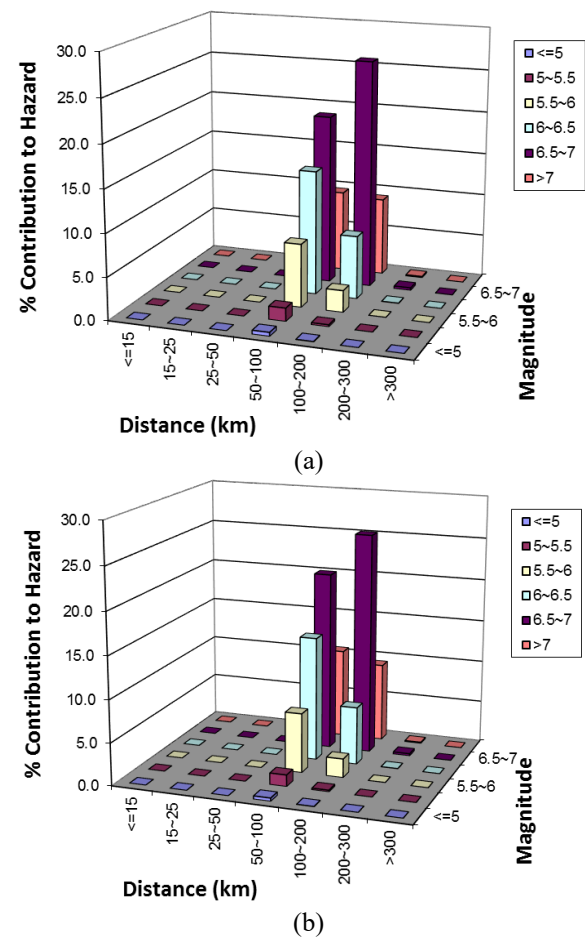

(a)

(b)

Fig. 6 Hazard deaggregation for weir structure site at two customary hazard levels: (a) 10% exceedance probability in 50 years and (b) 2% exceedance probability in 50 years

probabilities within 50 years for seismic source model A and B are 0.10 g and 0.13 g respectively.

Hazard deaggregation is a part of PSHA for analyzing the percentage of hazard contribution from certain size and location of the earthquake. 10% and 2% exceedance probabilities within in 50 years are two customary hazard levels recommended by Kramer (1996). Fig. 6 shows the respective PGA hazard deaggregation at the two hazard levels for source model A. As can be seen in the figure, 95%
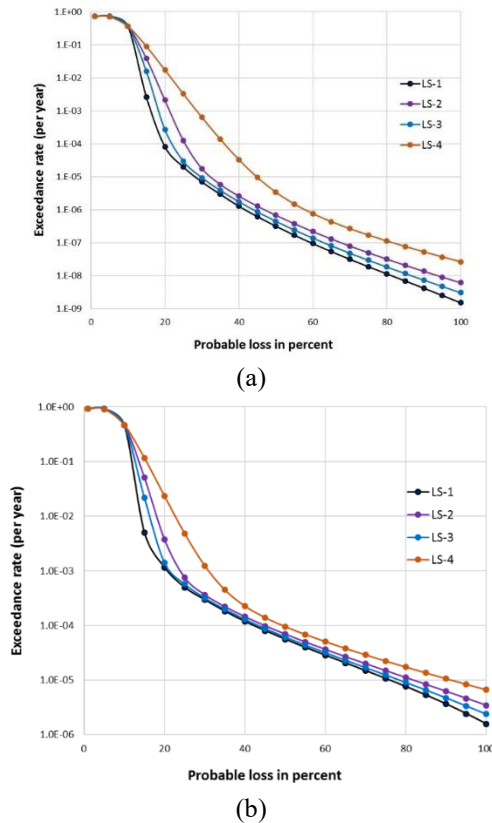
(a)

(b)

Fig. 7 Seismic risk curve of Gangjeong-Goreyeong weir structure: (a) for source model A, and (b) for source model B

different source models to quantify the seismic hazard for the weir site, and the results show a significant variation of hazard. The hazard deaggregation is extracted at two customary hazard levels. The deaggregation shows that most probable scenario of hazard for the weir structure site is contributed by magnitude (5.5-7.0M_w) and occurrence between 50 to 200 km from the weir site. The method for reckoning the annual probability of seismic risk corresponding exceedance rate is presented by incorporating the seismic hazard and fragility results. For future study related to monetary issues, the probable maximum loss (PML) as criteria for the estimation of economic loss can be calculated from the risk curve.

References

Alam, J., Kim, D. and Choi, B. (2017), "Uncertainty reduction of fragility curve of intake tower using bayesian inference and markov chain monte carlo simulation", *Struct. Eng. Mech.*, **63**(1), 47-53.

Ali, M., Alam, M., Haque, M. and Alam, M. (2012), "Comparison of design and analysis of concrete gravity dam", *Nat. Res.*, **3**(1), 18-28.

Ang, A.H.S. and Tang, W.H. (2006), *Probability Concepts in Engineering*, John Wiley & Sons, New York, U.S.A.

Arefian, A., Noorzad, A., Ghaemian, M. and Hosseini, A. (2016), "Seismic evaluation of cemented material dams-a case study of Tobetsu dam in Japan", *Earthq. Struct.*, **10**(3), 717-733.

Baker, J.W. (2013), *Probabilistic Seismic Hazard Analysis*, White Paper Version 2.0.1.

Baker, J.W. (2015), "Efficient analytical fragility function fitting using dynamic structural analysis", *Earthq. Spectr.*, **31**(1), 579-599.

Brabhaharan, P., Davey, R., O'Riley, F. and Wiles, L. (2005), *Earthquake Risk Assessment Study Part 1-Review of Risk Assessment Methodologies and Development of a Draft Risk Assessment Methodology for Christchurch*, Report No. U04/108: Final, Wellington, New Zealand.

Bradley, B.A. and Dhakal, R.P. (2008), "Error estimation of closed-form solution for annual rate of structural collapse", *Earthq. Eng. Struct. Dyn.*, **37**(15), 1721-1737.

Choi, I.K., Nakajima, M., Choun, Y.S. and Ohtori, Y. (2009), "Development of the site-specific uniform hazard spectra for Korean nuclear power plant sites", *Nucl. Eng. Des.*, **239**, 790-799.

Choi, I.K., Nakajima, M., Choun, Y.S. and Ohtori, Y. (2005), *Evaluation of the Current Seismic Zone of Korea Based on the Probabilistic Seismic Hazard Analysis*, KNS Spring Meeting.

Cornell, C.A., Banon, H. and Shakal, A.F. (1979), "Seismic motion and response prediction alternatives", *Earthq. Eng. Struct. Dyn.*, **7**, 295-315.

CRIEPI (2006), *Korea-Japan Joint Research on Development of Seismic Capacity Evaluation and Enhancement Technology Considering Near-fault Effect (Final Report)*, KAERI/RR-2688/2006.

of hazard are contributed by magnitudes (5.5-7.0M_w) and occurring between 50 to 200 km from site.

Eventually, the seismic risk of weir structure is assessed by integrating the seismic hazard probability and fragility function corresponding to the similar intensities. Fig. 7 shows the seismic risk curves of weir structure corresponding four different limit state for 2 seismic source model. As shown in this figure, the probable loss corresponding exceedance rate of weir structure for tensile stress of mass concrete (LS-4) is larger for both models. Moreover, the annual economic loss due to disruption of weir structure can be calculated from this figure.

7. Conclusions

This research quantified the risk of weir structures due to earthquake hazard in the Korean Peninsula. To assess the seismic vulnerability of weir structure, fragility functions are developed considering different four limit states (LS) of structural failure: compressive stress at weir body (LS-1), tensile stress at weir body (LS-2), compressive stress at mass concrete (LS-3) and tensile stress at mass concrete (LS-4). The structural fragility results are obtained from multiple time history analyses by using IDA method. The weir structure is found to be more susceptible to the tensile stress of mass concrete (LS-4) as compared to the other damage states. The PSHA approach is performed for two

Farzampour, A. and Kamali-Asl, A. (2015), "Seismic hazard assessment for two cities in Eastern Iran", *Earthq. Struct.*, **8**(3), 681-697.

FEMA (2001), *Earthquake Loss Estimation Methodology*, HAZUS99, Service Release 2, Technical Manual, Federal Emergency Management Agency, Washington, U.S.A.

Garcia-Mayordomo, J. and Insua-Arevalo, J.M. (2011), "Seismic hazard analysis for the Itoiz dam site (Western Pyrenees, Spain)", *Soil Dyn. Earthq. Eng.*, **31**, 1051-1063.

Gautam, D. (2017), "On seismic vulnerability of highway bridges in Nepal: 1988 Udaypur earthquake (MW 6.8) revisited", S*oil Dyn. Earthq. Eng.*, **99**, 168-171.

Gautam, D., Forte, G. and Rodrigues, H. (2016), "Site effects and associated structural damage analysis in Kathmandu valley, Nepal", *Earthq. Struct.*, **10**(5), 1013-1032.

Gutenberg, B. and Richter, C.F. (1944), "Frequency of earthquakes in California", *Bullet. Seismol. Soc. Am.*, **34**(4), 1985-1988.

Hariri-Ardebili, M.A. and Saouma, V.E. (2016), "Seismic fragility assessment of concrete dams: A state-of-the-art review", *Eng. Struct.*, **128**, 374-399.

Ibarra, L.F. and Krawinkler, H. (2005), *Global Collapse of Frame Structures under Seismic Excitations*, Report No. 152, John A. Blume Earthquake Engineering Center, Stanford, California, U.S.A.

Ju, B.S. and Jung, W.Y. (2015), "Evaluation of seismic fragility of weir structures in South Korea", *Math. Probl. Eng.*, **2015**, 1-10.

Kalantari, A. (2012), "Seismic risk of structures and the economic issues of earthquakes", *Earthq. Eng.*

Karaca, M.A. and Küçükarslan, S. (2012), "Analysis of dam-reservoir interaction by using homotopy analysis method", *KSCE J. Civil Eng.*, **16**(1), 103-106.

Kircher, C.A., Nassar, A.A., Kustu, O. and Holmes, W.T. (1997), "Development of building damage functions for earthquake loss estimation", *Earthq. Spectr.*, **13**(4), 663-682.

Kramer, S.L. (1996), *Geotechnical Earthquake Engineering*, Prentice Hall Inc., New Jersey, U.S.A.

McGuire, R.K. (1976), *FORTRAN Computer Program for Seismic Risk Analysis*, US Geological Survey, Open-File Report 76, 67.

McGuire, R.K. (1978), *FRISK Seismic Risk Analysis Using Faults as Earthquake Source*, US Geological Survey. Open-File Report 78, 1007.

Noroozinejad Farsangi, E., Hashemi Rezvani, F., Talebi, M. and Hashemi, S.A.H. (2014), "Seismic risk analysis of steel-MRFs by means of fragility curves in high seismic zones", *Adv. Struct. Eng.*, **17**(9), 1227-1240.

Pagni, C.A. and Lowes, L.N. (2006), "Fragility functions for older reinforced concrete beam-column joints", *Earthq. Spectr.*, **22**(1), 215-238.

Pitilakis, K.D., Anastasiadis, A.I., Kakderi, K.G., Manakou, M.V., Manou, D.K., Alexoudi, M.N., Fotopoulou, S.D., Argyroudis, S.A. and Senetakis, K.G. (2011), "Development of comprehensive earthquake loss scenarios for a Greek and a Turkish city: Seismic hazard, geotechnical and lifeline aspects", *Earthq. Struct.*, **2**(3), 207-232.

Porter, K. (2016), "A beginner's guide to fragility, vulnerability, and risk", *Encyclop. Earthq. Eng.*, 1-29.

Porter, K.A., Kennedy, R.P. and Bachman, R.E. (2006), *Developing Fragility Functions for Building Components*, Report to ATC-58, Applied Technology Council, Redwood City, California, U.S.A.

Seo, J.M., Min, G.S., Choun Y.S. and Choi, I.K. (1999), *Reduction of Uncertainties in Probabilistic Seismic Hazard Analysis*, KAERI/CR-65/99.

Tadinada, S.K. (2012), "A Bayesian framework for probabilistic seismic fragility assessment of structure", Ph.D. Dissertation, North Carolina State University, North Carolina, U.S.A.

Tekie, P.B. and Ellingwood, B.R. (2003), "Seismic fragility assessment of concrete gravity dams", *Earthq. Eng. Struct. Dyn.*, **32**, 2221-2240.

Vamvatsikos, D. and Cornell, C.A. (2002), "Incremental dynamic analysis", *Earthq. Eng. Struct. Dyn.*, **31**(3), 491-514.

Wang, J.P., Huang, D., Cheng, C.T., Shao, K.S., Wu, Y.C. and Chang, C.W. (2013), "Seismic hazard analyses for Taipei city including deaggregation, design spectra, and time history with excel applications", *Comput. Geosci.*, **52**, 146-154.

Zimmaro, P. and Stewart, J.P. (2017), "Site-specific seismic hazard analysis for Calabrian dam site using regionally customized seismic source and ground motion models", *Soil Dyn. Earthq. Eng.*, **94**, 179-192.

CC